A new surface recovery method based on hybrid reflectance model

Yanfeng Li [1*] Jiquan Ma [2]

[1] *Department of Information Science and Technology, Heilongjiang University,72 Xue Fu Road, Harbin, China*

[2] *Department of Computer Science and Technology, Heilongjiang University,72 Xue Fu Road, Harbin, China*

Received 6 October 2014, www.cmnt.lv

Abstract

Generally, the surface shape of a object can be recovered from a single image, that is called shape-from-shading (SFS), which relies on the assumption of Lambertian, although the specular reflectance component often exists in the original image. In order to improve the quality of the surface reconstruction in SFS, hybrid reflectance model is introduced firstly and is applied on SFS method. Firstly, the reflectance component is estimated using simulated annealing based on the distribution of the surface's normal. Secondly, a new surface recovery algorithm is designed under a hybrid reflectance model, which is a linear model composed with Lambertian and specular reflectance. Finally, Experiments are performed on synthetic and real images.

Keywords: Shape-from-shading; Hybrid Reflectance Model; Simulated Annealing

1 Introduction

3D reconstruction is a classic issue in the field of computer vision. 3D surface shape reconstruction is a technology, which uses one or more images of objects to obtain the three-dimensional surface shape information. Image brightness information is a very valuable clue for three-dimensional shape recovery. Using changes in the image brightness information, Horn of MIT proposed SFS technique, using brightness of a single image to achieve a three-dimensional surface shape information acquisition [1]. Compared with other three-dimensional reconstruction, SFS technology does not require complex equipment, has a good prospect in the production, life, medicine, meteorology, remote sensing and defence and military fields are tremendous value.

SFS is an ill-posed problem. Since 1970s, many SFS methods have been proposed, but due to the ambiguity of the images, the complexity of the imaging conditions and the cognitive process ambiguity for three-dimensional object. Precise three-dimensional shape of objects is recovered from single gray scale image is still a very difficult problem. Ref [2] and [3] have made a more complete classification and experimental comparison from a different perspective on the existing SFS algorithm, pointed out the flaws in each SFS algorithm, that is mainly reflected in the following aspects: (a) SFS algorithm is subject to the initial condition and prior knowledge, easy to fall into local minimum, even without the presence of convergence; (b) It is influenced greatly by the noise and their own shadows and less robust; (c) It has a higher computational cost, which is increasing with the image size, usually leads to the convergence speed too slow. Against defects and deficiencies solving SFS problem mentioned above, many universities and research institutions are studying how to improve the quality of SFS's recovery. Such as Professor Hancock York University research group led by the United Kingdom on the use of the cone of uncertainty to solve the SFS problem doing a series of studies [4-10], provides a new research ideas for SFS study. In California University, a universal SFS model under orthogonal projection and perspective projection is designed [11,12], which use Hamilton-Jacobi (HJ) and viscosity solution theory equations to solve the problem of SFS method. CVIP lab of Griffith University, in Australia, image pre-processing method for classical SFS algorithm is carried out in their research work, proposed removing the algorithm based on specular reflection and colour adjustment, reducing the impact of specular reflectance and colour changes on the surface shape recovery [13]. In Germany, MPI Informatik's C.Wu combined the multi-view stereoscopic methods and SFS methods. Firstly, stereo vision is used to restore the surface of the low-frequency component, and then use the information on the high-frequency details shading refinement; to solve multi-image SFS ambiguity caused by the error recovery. France Meryer of Lyon University, interaction model introduced in SFS algorithm allows users to interactively confirm the high light area is the peak or trough, regional non peaks and troughs of the non-use of mass-spring were interpolation, in order to

[*] Corresponding author's E-mail: liyanfeng@hlju.edu.cn

improve the applicability of SFS provides an effective way [15]; G.Zeng of Hong Kong University of Science and Technology also introduced the idea of interaction in face reconstruction process by SFS: face region is divided into a number of relatively small independent blocks and for each block, using conventional methods to recover the surface of the SFS, the entire surface of the end face region to give recovery of the results [16].

2 Shape-From-Shading based on hybrid model

2.1 IMPROVED TS ALGORITHM

Tsai and Shah proposed a linear SFS method. They used a first order centred differences for the expression of the directional gradient at each point of the surface. $p_{i,j}$ is defined as the gradient in x-axis; $q_{i,j}$ is defined as the gradient in y-axis. $z_{i,j}$ is the deep value at current point. The approximate $p_{i,j}$ and $q_{i,j}$ can be calculated by the upwind difference:

$$\begin{cases} p_{i,j} \approx z_{i,j} - z_{i-1,j} \\ q_{i,j} \approx z_{i,j} - z_{i,j-1} \end{cases} . \quad (1)$$

Based on this idea, a new radiation equation is obtained as the following:

$$R(p_{i,j}, q_{i,j}) = \frac{-s_x p_{i,j} - s_y q_{i,j} + s_z}{\sqrt{1 + p_{i,j}^2 + q_{i,j}^2}\sqrt{s_x^2 + s_y^2 + s_z^2}} . \quad (2)$$

The light source is given by the vector $S(s_x,s_y,s_z)$, the surface shape is represented by the surface normal vector at point (i,j).

From the equation (2), SFS can be looked as a PDE (Partial Difference Equation). Tsai and Shah proposed a linear algorithm by Taylor's expansion. We can find that this PDE relies on the the special light source condition, that is a unique light direction by a point light. When light setting is complex, this PDE cannot reach a accurate reconstruction, even leading to a error. In my article, a central differences are introduced, which can be defined as bellow:

$$\begin{cases} p_{i,j} \approx \frac{1}{2}\left[\frac{z_{i+1,j+1} - z_{i,j+1}}{h} + \frac{z_{i+1,j} - z_{i,j}}{h}\right] + o(h^2) \\ q_{i,j} \approx \frac{1}{2}\left[\frac{z_{i,j+1} - z_{i,j}}{h} + \frac{z_{i+1,j+1} - z_{i+1,j}}{h}\right] + o(h^2) \end{cases} . \quad (3)$$

Results calculated using the central difference is smaller than upwind difference. Due to the low-order intercept a number of poor-order upwind schemes, unless a fairly fine grid, the calculation results in large errors.

In our experiment framework, we set the camera in the direction $C(c_x,c_y,c_z)$. According the features of specular reflectance, we assume that the light is reflected by the surface and projected in the camera's direction. So, we calculated the the middle vertical line between light source and camera is defined as the vector $M((s_x+c_x)/2,(s_y+c_y)/2,(s_z+c_z)/2)$. Here, this is defined as $M(m_x,m_y,m_z)$.

In this article, we designed a new radiation equation that is expressed as follow:

$$\begin{aligned} R(p_{i,j}, q_{i,j}) = w_{i,j} * & \frac{-s_x p_{i,j} - s_y q_{i,j} + s_z}{\sqrt{1 + p_{i,j}^2 + q_{i,j}^2}\sqrt{s_x^2 + s_y^2 + s_z^2}} \\ & + (1 - w_{i,j}) * \left[\frac{-m_x p_{i,j} - m_y q_{i,j} + m_z}{\sqrt{1 + p_{i,j}^2 + q_{i,j}^2}\sqrt{m_x^2 + m_y^2 + m_z^2}}\right]^k . \end{aligned} \quad (4)$$

$\omega_{i,j}$ is the weight of reflectance component, here we only considered two types of reflectance (Lambertian and Specular reflectance); k is the factor for specular reflection, which describes its level.

As it is deduced by TS., the radiation equation can be rewritten as:

$$\begin{aligned} 0 &= f(I_{i,j}, Z_{i,j}, Z_{i-1,j}, Z_{i,j-1}) \\ &= I_{i,j} - R(Z_{i,j} - Z_{i-1,j}, | Z_{i,j} - Z_{i,j-1}). \end{aligned} \quad (5)$$

$I_{i,j}$ is the input intensity of the source image at point (i,j). Then Taylor expansion is used to the function f according to the equation (5), at a given depth map Z^{n-1}. So, a linear differential equation can be obtained as follows:

$$0 = f(Z_{i,j}) \approx f(Z_{i,j}^{n-1}) + (Z_{i,j} - Z_{i,j}^{n-1})\frac{d}{dZ_{i,j}} f(Z_{i,j}^{n-1}) . \quad (6)$$

According to above iteration, the next depth map at the n-th iteration can be deduced as follows:

$$Z_{i,j}^{n} = Z_{i,j}^{n-1} + \frac{-f(Z_{i,j}^{n-1})}{\frac{d}{dZ_{i,j}} f(Z_{i,j}^{n-1})} . \quad (7)$$

Here, $\frac{d}{dZ_{i,j}} f(Z_{i,j}^{n-1})$ is the first-order derivative about the depth, which is defined as:

$$\begin{aligned} \frac{d}{dZ_{i,j}} f(Z_{i,j}^{n-1}) = -\omega * & \left[\frac{p_s + q_s}{\sqrt{p^2 + q^2 + 1}\sqrt{p_s^2 + q_s^2 + 1}} - \frac{(p+q)(pp_s + qq_s + 1)}{\sqrt{(p^2 + q^2 + 1)^3}\sqrt{p_s^2 + q_s^2 + 1}}\right] - (1 - \omega) * \\ & k\left[\frac{p_h + q_h}{\sqrt{p^2 + q^2 + 1}\sqrt{p_h^2 + q_h^2 + 1}}\right]^{k-1}\left[\frac{p_h + q_h}{\sqrt{p^2 + q^2 + 1}\sqrt{p_h^2 + q_h^2 + 1}} - \frac{(p+q)(pp_h + qq_h + 1)}{\sqrt{(p^2 + q^2 + 1)^3}\sqrt{p_h^2 + q_h^2 + 1}}\right]. \end{aligned} \quad (8)$$

2.2 REFLECTANCE COMPONENT PROBABILITY

In the irradiation equation, diffuse reflectance and specular reflectance are the most important component. In hybrid model, the proportion of different reflectance components is described as probability of point (i, j) , which will make a minimization of the diversity between the ccalculated intensity value and the corresponding pixel gray-level in the source input image. Here, $I_{ds} = p((i,j) \in L) * I_d + p((i,j) \in S) * I_s$ is the simulated intensity value, Lambertian is described as the probability $p((i,j) \in L)$ and the specular reflectance is described as the probability $p((i,j) \in S)$, I_d, I_s respectively represents the calculated intensity corresponding the Lambertian and specular reflectance. Under this framework, using simulated annealing iteration

$I_{ds} = p((i,j) \in L) * I_d + p((i,j) \in S) * I_s$ converges to the intensity of the input image. Based on above idea, the algorithm is shown as follows:

Set original temperature T=T_m, Cycles is C,
probability factor is $\alpha = p((i,j) \in L)$, $\beta = p((i,j) \in S)$ 。
While (T>0)
Begin
For (k=1,2,……,C)
Begin
Add Disturbance:
$\alpha' = \alpha + r \times m$; $\beta' = \beta + r \times m$
// $r = random(0,1)$, m ***is step length***
Evaluation Function:
$V = \alpha \times I_d + \beta \times I_s$;
$V' = \alpha' \times I_d + \beta' \times I_s$
If $(\Delta t = (V - V') < 0)$
$\alpha = \alpha', \beta = \beta', V = V'$
Else
$\exp(\frac{\Delta t}{T}) > random(0,1)$
$\alpha = \alpha', \beta = \beta', V = V'$
End
Update Normal: $\overrightarrow{M}(i,j) = \overrightarrow{M}(i,j) * \alpha + \overrightarrow{N_s} * \beta$
Update Temperature: $T=\lambda T$, $0<\lambda<1$
End
Reflectance Probability of Surface Point :

$$p((i,j) \in L \mid E(i,j), \overrightarrow{M}(i,j)) = \alpha$$
$$p((i,j) \in S \mid E(i,j), \overrightarrow{M}(i,j)) = \beta$$

With this algorithm convergence, the proportion ω in the equation (8) can be obtained according to the reflectance probability. In order to keep the consistency, normalization is done to the reflectance probability using following equation:

$$\omega_{i,j} = \frac{p((i,j) \in L)}{Max\{p((i,j) \in L) \mid (i,j) \in \Omega)} . \quad (9)$$

3 Experiments

3.1 SAMPLE SELECTION AND PREPROCESSING

In our tests, we applied our new method on one simulated and two real images, which come from http://www.irit.fr/sfs . These synthetic images were obtained from a known simulated shape, which is computed on size $[-6.4,6.4]^2 \in \Re^2$ and mapped to a square image of 256×256 pixels, the coordinate size of the image is $d = 12.8/256 = 0.05$. The simulated shape (DEM in the following) is defined by:

$$DEM(x,y) = 3(1-x)^2 \exp(-x^2 - (y+1)^2) - 10(x/5 - x^3 - y^5) \times \exp(-x^2 - y^2) - 1/3 \exp(-(x+1)^2 - y^2) \quad (10)$$

From the Figure 1, we can see the 3D shape about the simulated data and the corresponding image.

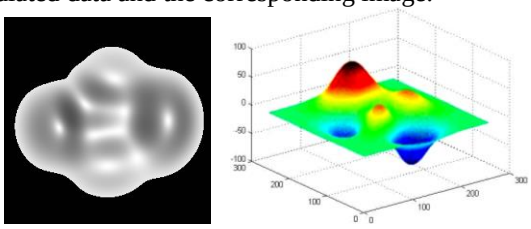

FIGURE 1 Synthetic image and its shape

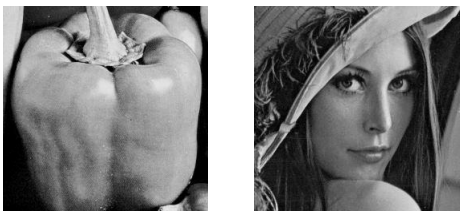

(a) (b)

FIGURE 2 Real images (a) Pepper and (b) Lena, no ground truth deep data with them

We select the Pepper and Lena image as the real data. Their sizes are all 256×256, and the ground truth depth is unavailable. Their size is considered as 12.8×12.8, under the assumption of the size proportion d is equal to 0.05. In Figure 2, (a) is the Pepper image; (b) is the Lena image.

3.2 TEST 1: DEM

In this test DEM is used as the input image. It is a synthetic image, which has been mentioned above (Figure 1). We compared the result about classical TS method and mine in Figure 3 and Figure 4. The left image is the reconstructed image from the recovered 3D shape as displayed as right mesh.

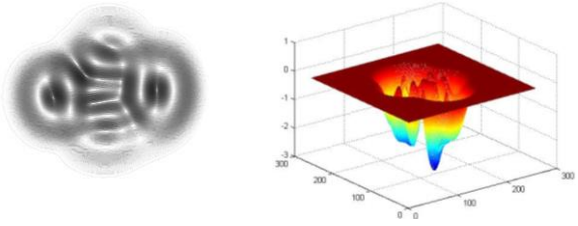

FIGURE 3 TS on DEM

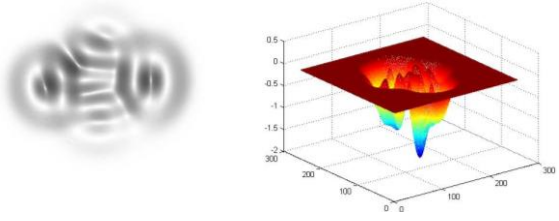

FIGURE 4. TS* on DEM

Evaluation about the performances of shape-from-shading is carried out. This evaluation include three parts: the first is the measurement of the deviation between the calculated deep data $\tilde{u}$ and the ground truth deep data u; the second part is to compare the input image intensity I with the estimated image intensity $\tilde{I}$, which is calculated from the reconstructed shape using radiation equation, especially for real images whose shapes are not available; the last part, when surface normal n is known for the real object's surface shape, it is essential to compare it with the estimated $\tilde{n}$. For DEM, the ground truth depth and normal is known, so we can get the mean absolute deviation error $|\Delta u|_1$, $|\Delta n|_1$, $|\Delta I|_1$; the root mean square error $|\Delta u|_2$, $|\Delta n|_2$, $|\Delta I|_2$ and the maximal absolute deviation error $|\Delta u|_\infty$, $|\Delta n|_\infty$, $|\Delta I|_\infty$.

TABLE 1 Errors on DEM

Ps=0.0,Qs=1.0,Iter=5,K=7									
DEM	$\|\Delta u\|_1$	$\|\Delta u\|_2$	$\|\Delta u\|_\infty$	$\|\Delta n\|_1$	$\|\Delta n\|_2$	$\|\Delta n\|_\infty$	$\|\Delta I\|_1$	$\|\Delta I\|_2$	
TS	0.64	0.94	2.93	0.67	0.81	1.77	0.12	0.17	
TS*	0.58	0.85	2.75	0.61	0.76	1.77	0.09	0.14	0.60

It will be found that the recovered surface are all existed big error in two SFS methods. In Table 1, the performance is shown by magnitude of the errors on the depth, normal and intensity. We can find that the improved algorithm TS* has better performance.

3.3 TEST 2: PEPPER AND LENA

For real image, complex reflection existed in it. The basic assumptions about SFS generally cannot be expected. And so on, ground truth depth is unavailable, but is considered as the classical benchmarks. So, the comparison only is made on the estimated image and the input image. From Table 2 and Table 3, we can find that the proposed TS* has better performance on $|\Delta I|_1$, $|\Delta I|_2$ and $|\Delta I|_\infty$. The accuracy is increased by about 6 percent.

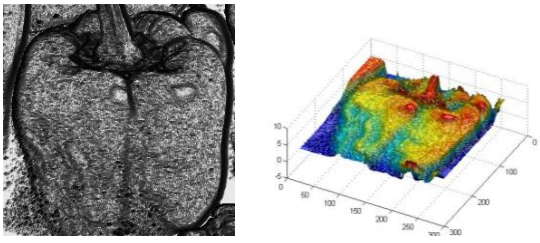

FIGURE 5. TS on Pepper

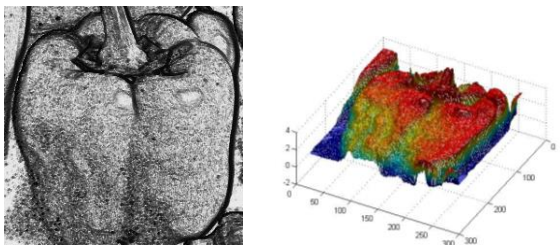

FIGURE 6. TS* on Pepper

TABLE 2 Errors on Pepper

Ps=0.0,Qs=1.0,Iter=5,K=7			
Pepper	$\|\Delta I\|_1$	$\|\Delta I\|_2$	$\|\Delta I\|_\infty$
TS	0.27	0.36	1.00
TS*	0.21	0.30	1.00

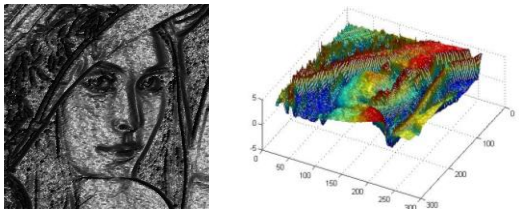

FIGURE 7. TS on Lena

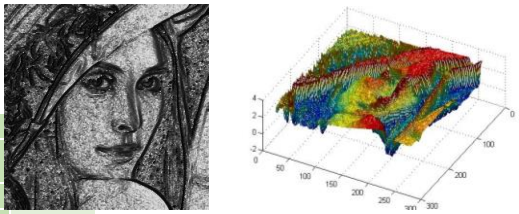

FIGURE 8. TS* on Lena

TABLE 3 Errors on Lena

Ps=0.0,Qs=1.0,Iter=5,K=7			
Lena	$\|\Delta I\|_1$	$\|\Delta I\|_2$	$\|\Delta I\|_\infty$
TS	0.25	0.31	0.95
TS*	0.21	0.26	0.91

4 Conclusion

A hybrid 3D surface reconstructed model using reflectance component estimation is introduced. A linear model according to the hybrid reflectance component is designed to reconstruct the the surface. This method provided an opportunity to recover the object's surface that does not meet the Lambertian assumption. At the same time, in the actual application, specular reflectance estimation and removal is a very important research point. The proposed de reflectance component estimation algorithm will be easily applied on image processing and computer vision produce. Experiment reveals that this method is viable and great help to the precision of the shape-from-shading.

References

[1] Horn B K P 1970 *Shape from shading:a method obtaining the shape of a smooth opaque object from one view* Massachusetts, MIT

[2] Zhang R, Tsai P S, Cryer J E, Shah M 1999 *Shape from shading:a survey* IEEE Transactions on Pattern Analysis and Machine Intelligence **21**(8) 690-706

[3] Durou J D, Falcone M,Sagona M 2008 *Numerical methods for shape-from-shading: A new survey with benchmarks* Computer Vision and Image Understanding **109** 22-43

[4] Worthington P L, Hancock E R 1999 *New constraints on data-closeness and needle map consistency for shape-from-shading* IEEE Transactions on Pattern Analysis and Machine Intelligence **21**(12) 1250-67

[5] *Deleted by CMNT Editor*
[6] Ragheb H, Hancock E R 2003 *Darboux smoothing for shape-from-shading* Pattern Recognition Letters **24**(1-3) 579-95
[7] Bors A G, Hancock E R, Wilson R C 2003 *Terrain analysis using radar shape-from-shading* IEEE Transactions on Pattern Analysis and Machine Intelligence **25**(8) 974-92
[8] Worthington P L, Hancock E R 2003 *Coarse view synthesis using shape-from-shading* Pattern Recognition **36**(2) 439-49
[9] Worthington P L, Hancock E R 2000 Histogram-based object recognition using shape-from-shading *IEEE Conference on Computer Vision and Pattern Recognition Hilton Head Island SC USA* **1** 643-48
[10] *Deleted by CMNT Editor*
[11] Prados E, Soatto S 2005 Fast Marching Method for Generic Shape from Shading *Lecture Notes in Computer Science* Berlin Springer-Verlag **3752** 320-31
[12] Prados E 2004 *Application of the theory of the viscosity solutions to the shape from shading problem* University of Nice sophia antipolis
[13] Zhang Xiaozheng, Gao Yongsheng, Caelli Terry 2010 *Colour Adjustment and Specular Removal for Non-Uniform Shape from Shading* Digital Image Computing: Techniques and Applications 563-68
[14] Wu C, Wilburn B, Matsushita Y, Theobalt C 2011 *High quality shape from multi-view stereo and shading under general illumination* CVPR 969-76
[15] *Deleted by CMNT Editor*
[16] Zeng G, Matsushita Y, Quan L, Shum H Y 2005 Interactive Shape from Shading *Proceedings of the IEEE Conference on Computer Vision and Pattern Recognition* **I** San Diego, California, USA 343–50

Authors

Yanfeng Li , 1974.05, Harbin City, Heilongjiang Province, P.R. China

Current position, grades: Engineer of Department of Information Science and Technology, Heilongjiang University, China.
University studies: received his B.Sc. in Computer Science and Technology from Heilongjiang University of Harbin in China. He received his M.Sc. from Northeastern University in China.
Scientific interest: His research interest fields include computer vision, image processing
Publications: more than 10 papers published in various journals.
Experience: He has teaching experience of 15 years, has completed five scientific research projects.

Jiquan Ma , 1975.11,Harbin City, Heilongjiang Province, P.R. China

Current position, grades: Associate professor of Department of Computer Science and Technology, Heilongjiang University, China.
University studies: received his B.Sc. in Computer Science and Technology from Heilongjiang University of Harbin in China. He received his M.Sc. from Harbin Institute of Technology in China. He received his D.Sc. from Harbin Institute of Technology in China.
Scientific interest: His research interest fields include computer vision, image processing, bioinformatics
Publications: more than 15 papers published in various journals.
Experience: He has teaching experience of 15 years, has completed six scientific research projects.